Rear wing rudiments

We're used to seeing rear wings on high-end single seaters incorporating complex features – but what about the fundamentals? We use CFD to go back to basics

By SIMON McBEATH

Winging it: harking back to a time when a rear wing was a much simpler device can teach us plenty about aerodynamics

Perhaps one of the reasons that rear wings in F1 and other senior (heavily regulated) single seater formulae incorporate complex details is that most of the basic design criteria are defined in the technical regulations. With limited or no freedoms on the fundamentals such as span, location and so forth, attention has to turn to more intricate features to try to extract performance advantages. But if some or all of these basic parameters are not already defined in technical regulations, where do you start, and what really matters? With the help of ANSYS CFD-Flo, a batch of simulations has been run on a single seater model to put some of the usual assumptions to the test. As ever, the picture is not as simple as those assumptions might have you believe.

Our model

Regular readers may recognise the CAD model **[CAD Figure 1]** that has been used for this latest investigation; it was utilised in our April 2014 feature 'Front wing fundamentals'. However, some changes have been made to the model to make it more generally applicable. The 2014 version was a design that had UK speed hillclimbing regulations in mind, and as such featured long rear diffuser tunnels extending well forwards, as well as the wide wing spans permitted in that category. This time the model featured a flat bottom between the wheels and a shorter diffuser. The front wing had a span of 1400mm with a part span flap either side of the nose, and it was moved 100mm closer to the front axle relative to the April 2014 study (which featured a dual element rear wing) to better balance the rear wing that was to be used in this exercise. The sidepod had been re-styled to eradicate some aero deficiencies seen in that 2014 study, notably some flow separation over the forward, upper parts and in the 'waist' ahead of the rear wheels. A 'bow divider' and splitter were added to the forward underbody to make the underbody flat between the wheels. And the baseline rear wing span was 1000mm, although other spans have been examined as one of the variables under investigation.

The author's usual ill-disciplined mix of imperial and SI units was employed, with air and ground speed in the simulations being 100mph (44.7m/s) and forces are reported in Newtons, N (divide N by 4.459 to obtain pounds, lb). The CFD simulations included mesh refinements around the wings and wheels for improved capture of flow separations; the K-epsilon turbulence model; moving ground; and rotating wheels. Each simulation was run until calculated forces were acceptably steady.

Wing data

It's common to see wings characterised by analysis in isolation, a useful means of providing information

AD Figure 1: The datum CAD model with single element, 1000mm span, 300mm chord ear wing. The racecar has been 'modified' for the purposes of this aerodynamic study

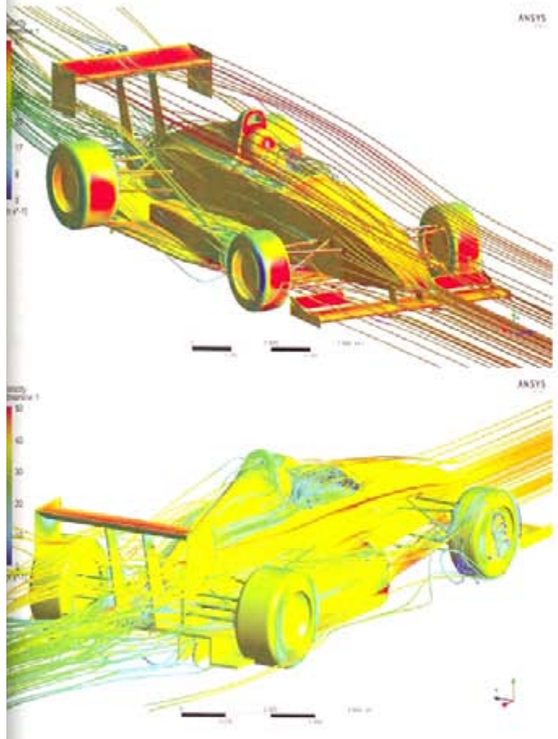

FD plots1 and 2: Rear wings operate in a highly compromised environment

Figure 2: Wing downforce in isolation versus the performance when fixed on the car

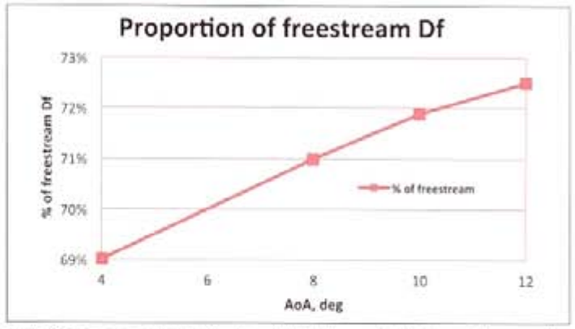

Figure 3: Rear wing made less downforce fitted to the car, but lost less at steeper angles

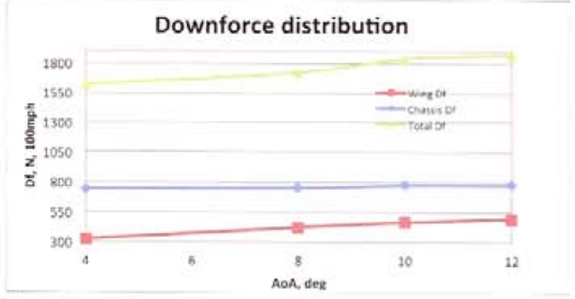

Figure 4: Not only the rear wing downforce increased as its angle was steepened

n a given wing's performance across n operating range, whether the formation has been divined in a ind tunnel or numerically (generally FD nowadays). Comparisons etween wings can also be done if he methodology and conditions are dentical. However, the performance of wing changes once it is affixed to a acecar, whatever type of car that may e, and that change in performance obviously very apparent when he car is a single seater. We saw in ur April 2014 study how front wing erformance was significantly altered y the presence of wheels and the st of the car downwind. Clearly hen we should expect that rear wing erformance will be much affected y the presence of most of the car and all four wheels upwind. However, it is also well-known that the rear wing can influence the aerodynamic performance of the upwind car. In essence then, this article explores how this rear wing was affected by its deployment on our single seater model, and in turn how the car was affected by the wing's deployment. **[CFD plots 1 and 2]**

The wing itself was a high downforce 300mm chord single element design with a relatively thin section and quite high camber. Chord remained fixed at 300mm in this study, purely on the basis that, in real-world practical terms, parameters like span and location are much more easily altered than section profile. It is hoped to continue with further on-car studies on variable wing chord and profile as well as dual- and multi-element designs in a future issue.

Angles

Generally the first means of characterising a wing is to carry out an 'alpha sweep', by mapping downforce versus angle of attack (AoA). So the wing was mapped in isolation across a working range, and the same sweep was repeated on the car. Span was 1000mm in each case. **Figure 2** plots wing downforce versus angle and, as would be expected, the downforce the wing made on the car was less than it made in isolation across the angle range. The shape of the downforce curve was very similar in both cases, with gains tailing off at the steeper angles. And although the gap between the two curves superficially appeared to grow with each steeper angle, in reality the proportion of freestream downforce that the wing made on the car (at this wing span and location) actually increased with angle, as shown by **Figure 3**.

Looking at the overall aerodynamic performance of the car across the wing angle range, **Figure 4** plots total downforce along with wing downforce and 'chassis' downforce. The latter included the chassis, bodywork, suspension, and importantly, the underbody, but excluded the wheels and the front wing. Total downforce, as would have been measured in a wind tunnel, increased with each wing angle

The performance of a wing changes once it is affixed to a racecar

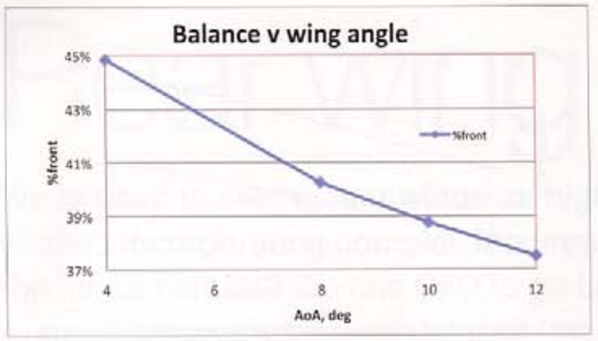

Figure 5: The balance responded to the rear wing angle change, as was expected

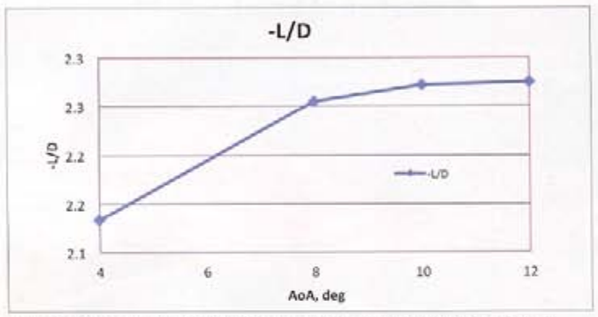

Figure 6: This shows that efficiency increases tailed off with increasing wing angle

Table 1 – the car's data across the rear wing angle range, forces in Newtons at 100mph

AoA, degrees	Drag	Downforce	%front	L/D
4	757.56	1615.60	44.81%	2.133
8	763.32	1720.91	40.24%	2.255
10	808.32	1836.01	38.74%	2.271
12	821.53	1868.22	37.48%	2.274

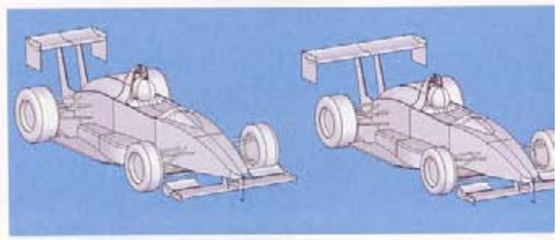

CAD-2: Rear wing spans from 800mm to 1400mm were evaluated on the racecar

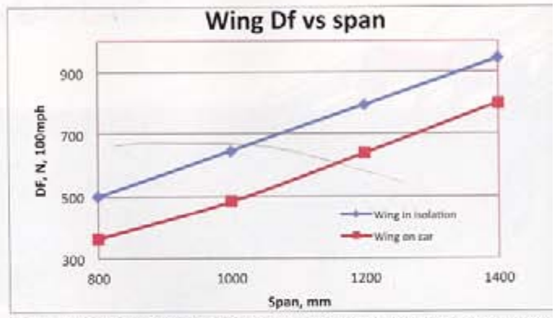

Figure 7: The wing's downforce gains as span was increased were greater on the
than on the wing in isolation – because of the driver etc., upstream of the centre se

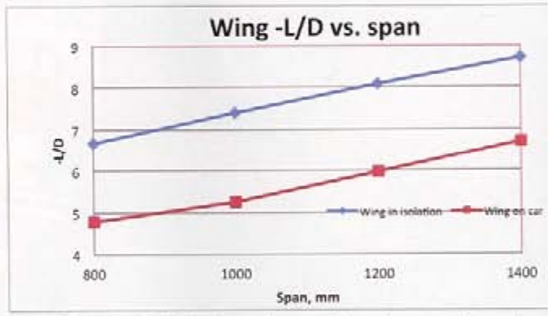

Figure 8: The wing's –L/D also improved more with span increases when on the c

increase, but notice the upwards step at 10 degrees. Exploiting the CFD to quantify the force contributions of individual component groups, it was evident that the chassis/underbody showed a modest step increase in downforce at 10-degree angle too. And not shown on this plot but which made a contribution here, wheel lift also appeared to reduce at the steeper wing angles, demonstrating simulated interactions that would not have been individually discernible in a wind tunnel that simply measured wheel contact forces (although a wind tunnel that supported the wheels separately from the chassis would pick that component up). The key point here is that yes, the rear wing's downforce contribution increased with increasing angle, as would be expected, but there were also other interactions, albeit it modest ones, in this opening example, that demonstrated the picture is rarely simple.

Figure 5 plots the car's aerodynamic balance (as '%front') versus wing angle and clearly showed the expected rearwards shift in balance with increasing rear wing angle. **Figure 6** plots –L/D (aerodynamic efficiency) versus wing angle, and shows that efficiency flattened off at the steeper wing angles. Together with the tailing off 'alpha sweep' plot, this suggested that the wing was approaching its maximum useful angle, in this application and configuration, at 10 degrees. **Table 1** summarises the data over the wing angle range tested.

Span decks

The baseline wing on which the alpha sweep was conducted had a span of 1000mm. It was decided to test some different spans at just one angle of attack, and the 10 degree AoA model from above was modified to spans of 800mm, 1200mm and 1400mm. The datum of 1000mm was chosen to represent the rear wing width limit seen in many a circuit racing category, while 1400mm is the UK's hillclimb maximum rear wing width. The narrower span of 800mm was chosen to see how narrow wings such as Formula 1 use would fare on the back of a 'regular' single seater. The wings were again tested in isolation and on the car. **(CAD Figure 2)**

When tested in isolation, the wing's downforce and drag both showed linear increases over the range of spans tested. Efficiency, as defined by –L/D (or downforce divided by drag) also increased linearly across this span range, too, which fitted with the accepted wisdom that efficiency improves as 'aspect ratio' (span divided by chord) is increased.

However, when the wing was located on the car the downforce gains that accrued with each span increment increased each time, the curve 'accelerating' slightly as span was increased **(see Figure 7)**. This reflects the fact that the central section of the wing was the most adversely affected when the wing was placed on the car, being behind the upstream obstruction of driver, roll hoop and so forth, whereas the additional widths are always in 'cleaner' air. –L/D plot of the wing in isolation versus on the car **(Figure 8)** sho similar picture. The wing clearly a lower -L/D when on the car, bu gains with each span increase g bigger each time, reflected in th proportion of freestream downf that the wing made on the car a angle and location, seen in **Figu**

The global picture is equally interesting. Overall downforce (drag) increased with increasing wing span, of course, but the ga tailed off at the top end of the s range, in contrast with the gains the rear wing itself and from the chassis/underbody **(see Figure** both of which actually saw sligh 'accelerated' gain at the widest This reflected an increase in wh lift at the widest span (reversing what was a decline in wheel lift each previous span increase), w coincided with the rear wing nc

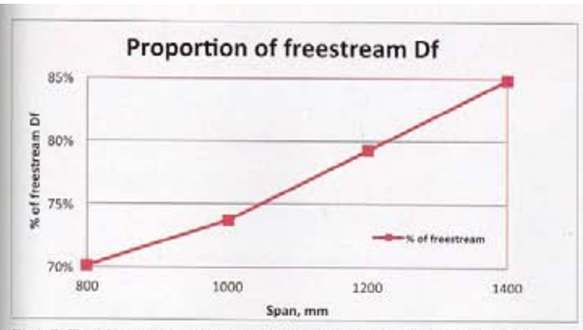

Figure 9: The wing lost a lot less of its 'in isolation' downforce at the larger spans

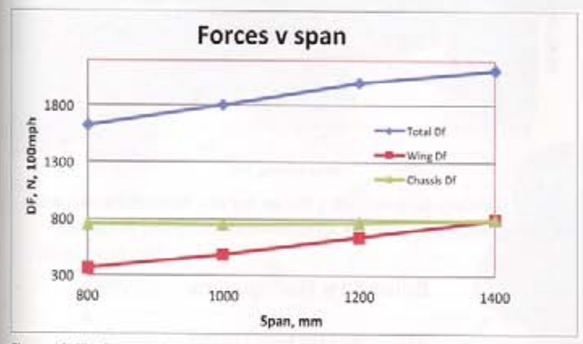

Figure 10: The increase in total downforce tailed off as the span was increased, this was despite wing and underbody downforce increases that did not tail off

Table 2 - the car's data across the rear wing span range, forces in Newtons at 100mph

Span, mm	Drag	Downforce	%front	L/D
800	762.32	1621.75	43.40%	2.127
1000	797.60	1804.91	38.34%	2.263
1200	824.52	1999.35	33.07%	2.425
1400	845.08	2111.40	28.01%	2.498

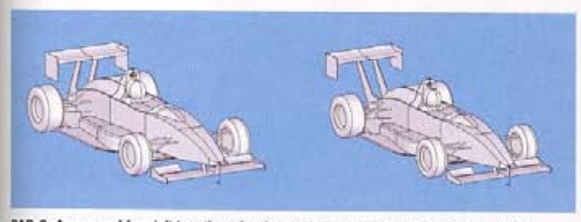

CAD-3: A range of fore/aft locations for the model's rear wing was also evaluated

being wider than the inside of the wheels and as such accelerating the airflow (and thus reducing the static pressure) over the tops of the tyres both front and rear. Balance not unexpectedly showed a marked and linear shift to the rear with each extra increment of rear wing span. **Table 2** summarises the data over the span range tested. Nevertheless, the downforce and efficiency gains certainly point towards using the maximum permitted span.

Fore/aft location

The datum fore/aft, or x-location in the forgoing sections, put the wing's leading edge at x=3.55m, where x=0 coincided with the tip of the car's nose. Three other x-locations for the wing were evaluated on the car, at 3.75m, 3.35m and 3.15m, the last of which put the wing's leading edge directly above the rear axle. These runs were with wing at 12 degrees, and **Table 3** summarises the data. **(CAD 3)**

Superficially this all looks fairly straightforward, with downforce and –L/D peaking at the datum fore/aft location of x = 3.55m, which we might naturally assume was where the wing interacted best (at this height) with the car's underbody. Balance, however, changed in an essentially linear fashion with the wing's fore/aft location, and we might simply assume that this was just down to the wing's location. However, check out **Figure 11** showing the downforce contributions of the rear wing and the chassis/underbody and it becomes clear that the picture is not that simple. Wing downforce actually peaked at the furthest forward location, which initially seemed curious but can be explained by **CFD plot 3 and 4** showing generally higher velocity in the airflow approaching the underside of the wing at x=3.15m. At the other locations the wing's

Table 3 – the car's data at different rear wing fore/aft locations, forces in Newtons at 100mph

x, m	Drag	Downforce	%front	L/D
3.15	833.30	1741.75	42.56%	2.090
3.35	820.24	1804.94	40.61%	2.201
3.55	821.53	1868.22	37.48%	2.274
3.75	807.65	1815.50	35.90%	2.248

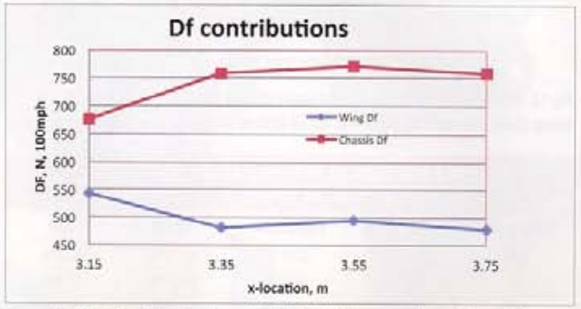

Figure 11: This shows the downforce contributions of the rear wing and chassis/underbody at varying wing fore/aft positions – and some interesting interactions

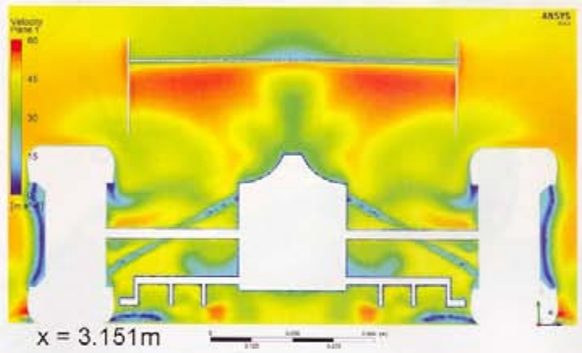

CFD-3: The velocity plot on the plane at the wing's leading edge at location x=3.15m shows 'freestream velocity plus' across most of the span

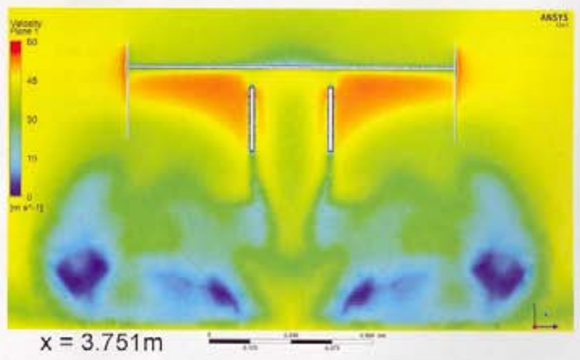

CFD-4: The velocity plot on the plane at the wing's leading edge at location x=3.75m shows lower velocities approaching the wing's all-important underside region

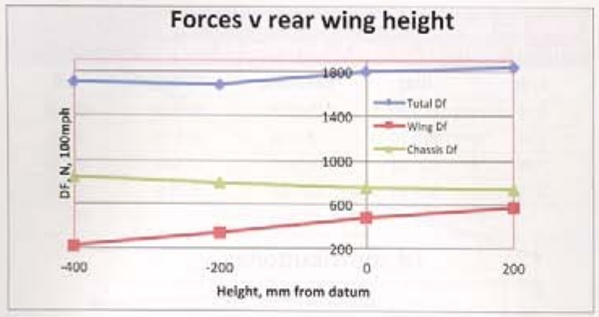

Fig 12: Adjusting rear wing height once again showed that interactions were taking place. The racecar model was tested at three additional wing heights

Table 4 – the car's data at different rear wing heights, forces in Newtons at 100mph

Delta y, mm	Drag	Downforce	%front	L/D
200	792.49	1835.17	35.17%	2.316
0	797.60	1804.91	38.34%	2.263
-200	757.51	1683.35	44.25%	2.222
-400	730.02	1699.86	48.06%	2.329

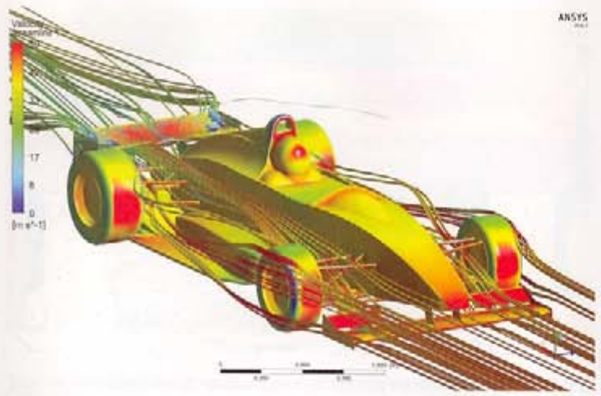

CFD-5: The rear wing's operating environment is much compromised at reduced height, but the car's overall aerodynamic performance didn't necessarily suffer

downforce was somewhat lower and altered little. Conversely, the chassis/underbody's downforce contribution increased significantly when the wing was moved from its furthest forward location and continued to increase to the datum position of x = 3.55m. So, while our initial assumption about interaction with the underbody looks correct, once more the detail shows a more complex situation.

Height

The datum height of the wing was initially set so that the top of the end plate, which was just clear of the top of the wing's trailing edge, was 900mm above ground, a typical maximum height in many single seater categories. Using the datum x-location of 3.55mm and AoA of 10 degrees the car was re-tested at three additional heights of +200mm, datum height. Overall drag and downforce, plus rear wing and chassis downforce are plotted in **Figure 12** and **Table 4** summarises overall data.

Overall drag was roughly the same at +200mm and datum height, but dropped fairly linearly by a modest amount at each of the next two lower heights. Overall downforce peaked with the rear wing at +200mm but recovered slightly when the wing was set at -400mm despite the initial decline with reducing height. Rear wing downforce showed a more or less linear decrease with each reduction in height, while conversely chassis/underbody downforce showed a more or less linear increase as wing height reduced. Not shown here, rear wheel lift also decreased with this last rear wing height reduction, this also contributing to the recovery in total

Table 5 – the car's data at different rear wing dual tier spacings

Tier spacing, mm	Drag	Downforce	%front	L/D
0	816.11	2033.74	33.78%	2.492
150	896.50	2248.07	28.02%	2.508
300	906.72	2211.00	28.59%	2.438
450	875.05	2209.92	33.84%	2.525

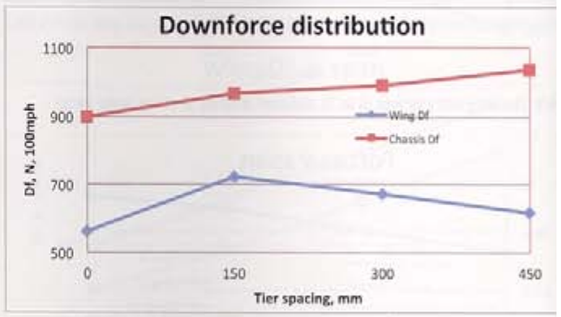

Figure 13: Downforce distribution with a dual tier rear wing fitted to the racecar mo and varying heights of the lower tier, again showed wing/underbody interactions

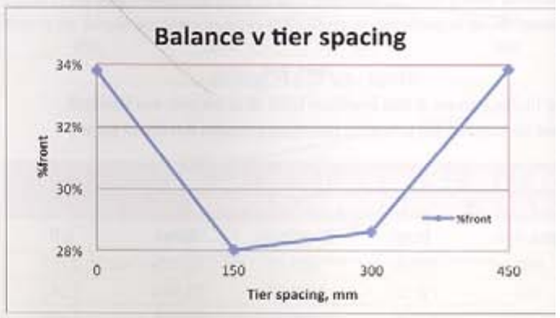

Figure 14: The balance was the same at the lowest second tier height as it was with no second tier, but the total downforce was greater in this configuration

Once more our immediate conclusion must be that the rear wing, despite generating less downforce itself, was interacting with the underbody more at lower heights and helping to increase the downforce of the latter **(CFD plot 5)**.

The –L/D shows that the initial decline with reducing wing height also sharply reversed at the lowest wing height, reflecting the relative efficiency of underbody generated downforce and also that overall drag had declined at the two lowest wing heights evaluated.

Multiple tiers

Additional tiers are a common sight on rear wings across a multitude of categories, although generally speaking the maximum is two tiers. Joseph Katz showed us in *Race Car Aerodynamics* (1st Ed.) that, in isolation, up to four tiers incrementally increased downforce potential but that the –L/D also incrementally

not recommended unless maxim downforce was sought and drag penalties were to be disregarded. of the problem is that space on th back of a racecar is usually limited by: regulatory maximum height; locating the lower tier to interact favourably with the diffuser exit; and physical space. Furthermore, Katz showed that putting one wir below or above another saw then interact unfavourably with each other and reduce the downforce each element, although the poter combined downforce could still b greater than a single wing on its c as long as vertical spacing betwee them was approximately 50 per c of chord or more.

With all the above in mind, du tier configurations were evaluate initially on our single seater mode at three different tier spacings; th lowest second tier position was 450mm below the datum height, which put the lower tier nicely ab

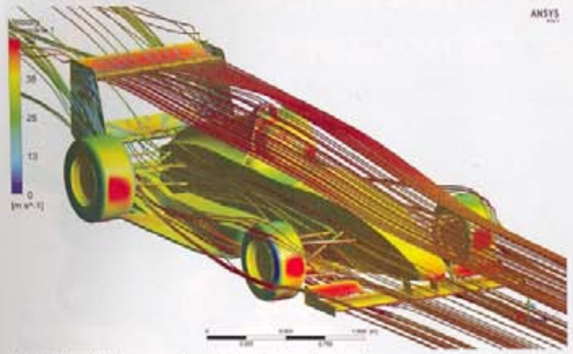

CFD-6: The dual-tier rear wing configuration worked well on our racecar model

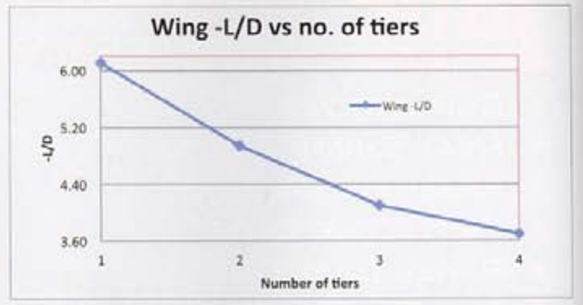

Figure 16: The –L/D of the wing assembly on the car showed an exponential decline with additional tiers

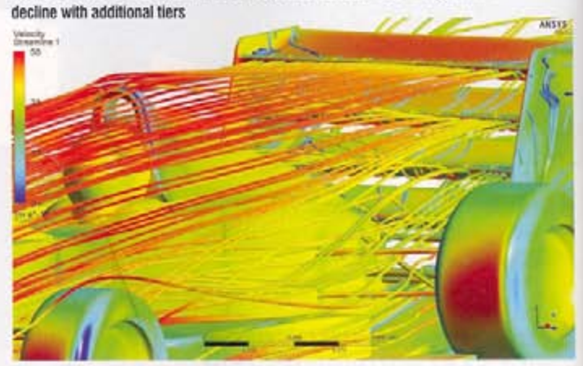

CFD-7: The airflow to each successive lower tier can be seen here to be compromised more than the one above. Yet multiple tiers can offer potential performance advantages, though that depends very much on the application. This is similar to the Katz plot

Table 6 – the car's data with one to four wing tiers

No. of tiers	Drag	Downforce	%front	L/D
1	816.11	2033.74	33.78%	2.492
2	875.05	2209.92	33.84%	2.525
3	959.52	2362.89	26.47%	2.463
4	1008.76	2487.99	24.50%	2.466

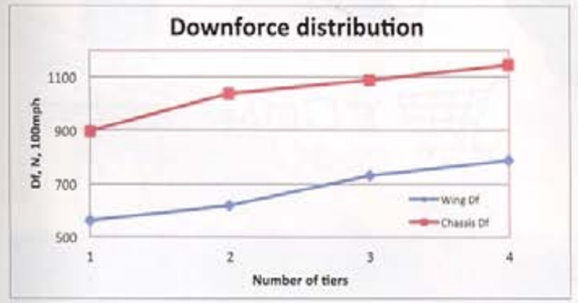

Figure 15: This graphic shows that the wing and the chassis/underbody downforce increased as the rear wing tiers were added to our racecar model

spacing was 300mm below the datum (= one chord's distance) and the highest position was 150mm below datum height. The upper tier was fixed at datum height, 10 degree AoA and x=3.55m in all cases. The second tier was set at the same angle and x-location. To connect the tiers the central mountings were replaced with end plate mountings that attached to the outside of the diffuser.

The overall results are shown in **Table 5**, and where the tier spacing is stated as 0mm only one tier was present, in the datum location, with end plate mountings.

Adding the second tier at 150mm (half a chord's distance) below the datum wing added slightly more than 10 per cent total downforce and also added just under 10 per cent more drag, which saw the –L/D value increase very slightly. Balance shifted rearwards fairly significantly.

However as the second tier's height was reduced, drag initially climbed slightly further but then reduced again, while downforce dropped and then stabilised over the next two spacings. Interestingly, but not entirely surprisingly given what we saw above when the single rear wing was lowered in height, when the second tier was put 450mm below the top tier the balance shifted forwards again and –L/D reached its maximum. The plots in **Figures 13 and 14** illustrate how the wing and chassis/underbody individually fared, and how balance changed. **Figure 13** shows the initial (29 per cent) jump in the wing assembly's downforce with the addition of the second tier, which then decreased at the next two lower positions as the lower wing tier was moved into what we know from the previous section was a less favourable environment. Chassis/underbody downforce, however, increased with the initial fitment of the second tier and continued to increase as that tier was lowered in height.

So locating a second wing tier 1.5 chord's distance below the upper tier increased total downforce by 8.7% and –L/D by 1.3% without changing the aerodynamic balance. On the downside drag increased by 7.2%, so the suitability of this configuration would obviously depend on the specific application **(CFD plot 6)**.

If placing the second tier 450mm below the first tier was the best solution from the above trial, and 450mm was accepted as the lowest practical location here, what would happen if one or two more tiers were fitted in between the top and bottom tiers? While this might be less practical if deeper section (for example multi-element) wing tiers were being used, with the relatively thin section single element wing here it was a simple thing to try. So one and two additional tiers were installed at even spacings between the top and bottom tiers, and the overall results are in **Table 6**.

A glance at **Table 6** shows that both downforce and drag increased roughly linearly with each additional tier and balance shifted rearwards with tiers three and four. It might be tempting to think that the extra intermediate tiers added drag and rear wing downforce only, but **Figure 15** shows that chassis/underbody downforce did respond to these intermediate tiers and contributed to the incremental downforce increases, just not by enough to prevent the balance shifting rearwards. Interestingly, the decrease in the car's –L/D with each extra tier was very modest in the context of the whole car, although plotting the –L/D of the wing assembly only versus the number of tiers **(see Figure 16)** produced a generically similar plot to that published by Katz. **(CFD plot 7)**

Summary

This brief look of some of the rudiments of rear wings has highlighted that simple assumptions can hide some of the detail of what is actually going on. But CFD can reveal useful and fascinating insights into the underlying interactions.

Many thanks to ANSYS UK for providing the CFD software.

Simple assumptions can hide some of the detail of what is going on